Progress In Electromagnetics Research C, Vol. 53, 155–163, 2014

A Printed Dual-Band Dual-Sense Circularly Polarized Metal-Strip Antenna with Double Split-Ring Elements

Guowei Zhang[1, *], Fushun Zhang[1], Yali Yao[1], Li Jiang[1], and Qichang Li[2]

Abstract—A novel and simple dual-band dual-sense circularly polarized (CP) metal-strip antenna is proposed. The antenna fed by a coplanar waveguide (CPW) with the advantages of uniplanar geometry and easier fabrication consists of a square slot and two split-ring elements. By appropriately introducing dual split-ring elements, the proposed dual-band CP design can easily be achieved. The two resonant frequencies are controlled by the size of the two split-ring elements. The proposed antenna prototype is fabricated and measured. Experimental results show that good CP radiation performances are obtained at both resonant frequencies. The proposed antenna has an impedance bandwidth ($|S_{11}| \leq -10\,\mathrm{dB}$) of 63.3% ($2.0 \sim 3.9\,\mathrm{GHz}$), and the dual band circular polarization with left hand circular polarization (LHCP) at 2.2 GHz and the right hand circular polarization (RHCP) at 3.8 GHz are obtained. Also, the 3-dB axial ratio bandwidths are about 220 and 190 MHz at the lower and upper band, respectively.

1. INTRODUCTION

In recent years, there has been increasing demand for antennas for higher transmission capacity. An effective way is to utilize an antenna with orthogonally CP at two discrete operating frequencies. The reason is that incoming waves of any polarization can be received by a right-hand circularly polarized (RHCP) antenna except the one of left-hand circular polarization (LHCP), and vice versa. Therefore, the antenna operating frequency can be reused to enlarge the overall capacity in the wireless transmission. Dual-band dual-sense CP antennas become a popular study in this research area during the last few years. Several dual-frequency designs for antenna structures have been proposed in [1–11], including slot antenna, notched printed monopole antenna, multifunction hybrid antenna, dual-feed antenna arrays.

For generating circular polarization (CP) radiation using a single feed, many microstrip antenna designs have been reported [12, 13]. The obtained CP bandwidth (3-dB axial-ratio bandwidth), however, is usually narrow and less than 2%. When the same microwave substrate is used, corresponding printed slot antennas, especially wide slot antennas [14–20], usually have a much wider CP bandwidth than single-feed ones. The CP bandwidth of about 12% has been achieved for a microstrip line-fed square slot antenna [15], and it is also noted that most of the available circularly polarized wide slot antenna designs are with a microstrip line feed [14–19]. The design with a CPW feed [20–24] is widely used to obtain broadband, as it is known that printed slot antennas with a CPW feed have the advantage of uniplanar geometry and are thus easier to fabricate than the design with a microstrip line feed. However, in the past, most of slot CP antennas have been shown to achieve wider bandwidths in both impedance and AR only at a single band. It was rare for slot CP antennas to achieve broad bandwidths in both impedance and AR simultaneously at the two operating bands using a single-layer and single-feed configuration. In addition, its radiation pattern is distorted with the asymmetric structure at the upper band. This motivates the present study.

Received 9 July 2014, Accepted 19 September 2014, Scheduled 25 September 2014
* Corresponding author: Guowei Zhang (gwzh0424@163.com).
[1] National Laboratory of Science and Technology on Antennas and Microwaves, Xidian University, Xi'an, Shaanxi 710071, China.
[2] North Electro-Mechanical Intelligent Technology Corporation Limited, Beijing 101149, China.

The proposed dual-band dual-sense CP metal-strip antenna with novel configuration consists of a square slot and two split-ring elements as shown in Fig. 1. The outer ring is connected with CPW at the corner to generate two orthogonal modes to perform CP radiation at the lower band. By employing another split-ring which is coupling fed by the outer one, the upper CP radiation resonant frequency is obtained. The two operating bands can be controlled by the size of the two rings. The introduced split-ring contributes to both dual-frequency CP operation and bandwidth enhancement. The results of the proposed antenna are compared with those of recent works in [25–27]. As shown in Table 1, relatively advantageous results have been observed with a size of only 50 mm by 50 mm. Details of the antenna design are described, and prototypes of the proposed antenna have been constructed and tested. Section 2 shows the structure of this antenna and discusses the mechanism of this antenna. Section 3 and Section 4 show the simulated and measured results of this antenna and the parametric study.

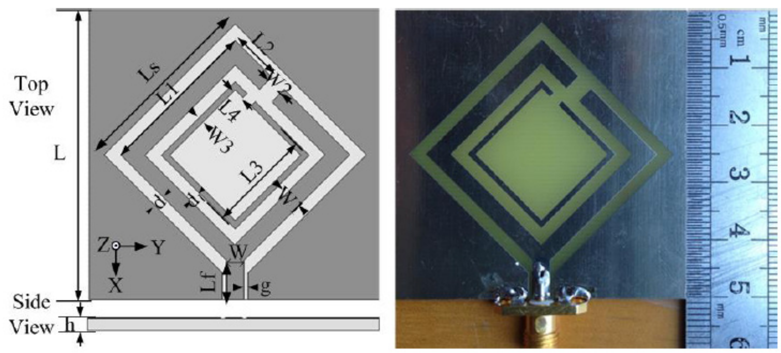

Figure 1. Geometry of the proposed antenna.

Table 1. The comparison on the performance of the proposed antenna.

Refs.	Impedance bandwidth	3 dB axial ratio bandwidth	Radiation pattern	Antenna size (mm)
This work	$2.0 \sim 3.9$ GHz (1.9 GHz, 63.3%)	220 MHz (2.2 GHz 10%) 190 MHz (3.8 GHz 5.0%)	distortionless (lower band) distortionless (upper band)	$50 \times 50 \times 2$
[25]	$1.45 \sim 1.72$ GHz (270 MHz, 17%) $1.86 \sim 2.29$ GHz (430 MHz, 21%)	$1.47 \sim 1.61$ GHz (140 MHz, 9.0%) $1.89 \sim 2.09$ GHz (200 MHz 10%)	distortionless (lower band) distorted (upper band)	$70 \times 70 \times 1.6$
[26]	$2.28 \sim 2.66$ GHz (380 MHz, 15.4%) $3.76 \sim 3.95$ GHz (190 MHz, 5.0%)	$2.36 \sim 2.45$ GHz (90 MHz, 3.7%) $3.76 \sim 3.83$ GHz (70 MHz, 1.9%)	distortionless (lower band) distortionless (upper band)	$60 \times 60 \times 8$
[27]	$2.1 \sim 2.7$ GHz (600 MHz, 24%) $5.5 \sim 7.1$ GHz (1.6 GHz24%)	$2.42 \sim 2.57$ GHz (150 MHz, 5.9%) $6.42 \sim 6.58$ GHz (160 MHz, 2.46%)	distortionless (lower band) distortionless (upper band)	$50 \times 30 \times 1.45$

2. ANTENNA DESIGN

As shown in Fig. 1, the proposed antenna is fabricated on a substrate of thickness 2 mm with a dielectric constant of $\varepsilon_r = 4.4$ and a loss tangent of 0.02. The antenna consists of a square slot and two split-ring elements. A rotated split-ring is connected to the CPW. In detail, by optimizing the location of the gap embedded in the rotated ring, two orthogonal modes with 90 phase difference is generated to excite circular polarization at the lower band (LHCP). One of the main goals of the design is to create dual-band dual-sense circular polarization. Hence, an inner split-ring is employed to obtain the upper CP radiation resonant frequency. As is coupling fed by the split-ring feeding line, the inner ring has a surface current out of phase with that of the outer one. Thus, an opposite CP radiation is produced at the upper band (RHCP). The optimal dimensions of the designed antenna are specified in Table 2.

Table 2. Optimum parameters of the proposed antenna (unit: mm).

L	L_1	L_2	L_3	L_f	L_s	L_4
50	28	9	18	6.7	32	2
W	W_1	W_2	W_3	d	g	d_1
3	3	3	1	2	0.7	2

At first, to clarify the improvement process, two antenna prototypes are defined as follows in Fig. 2. Ant 1 includes a square slot and a split-ring feeding line with a length L_1 of 28 mm, which is close to $\lambda_g/4$ at the lower band (2.2 GHz). An added inner split-ring with a length L_3 of 18 mm, which is close to $\lambda_g/4$ at the upper band (3.8 GHz) is employed in Ant 2 to obtain the upper CP radiation resonant frequency.

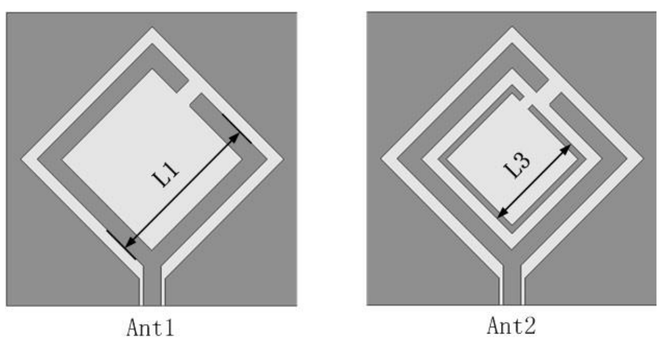

Figure 2. Two improved prototypes of the proposed antenna.

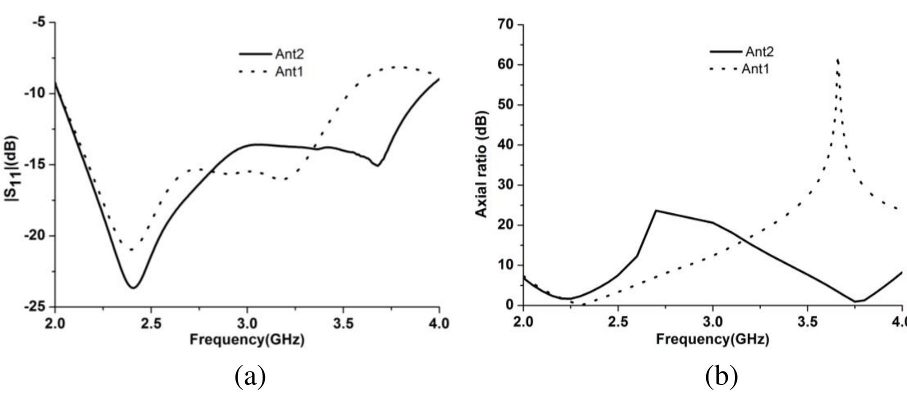

Figure 3. Simulated $|S_{11}|$ and AR for Ant 1 and Ant 2, (a) $|S_{11}|$, (b) AR.

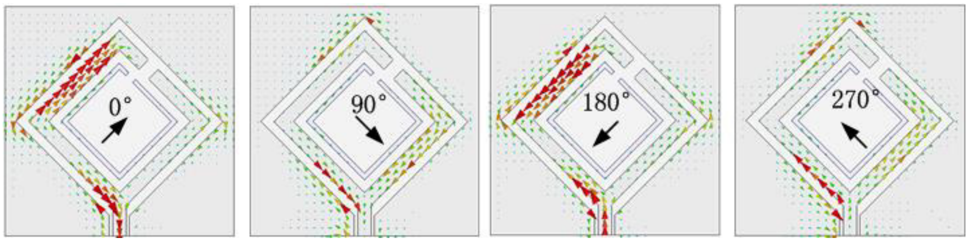

(a) 2.2 GHz

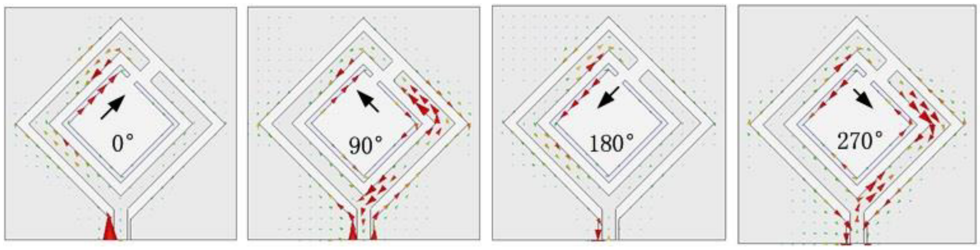

(b) 3.8 GHz

Figure 4. Surface current distributions of the proposed antenna 2 in 0°, 90°, 180° and 270° phase. (a) 2.2 GHz. (b) 3.8 GHz.

Comparisons between Ant 1 and Ant 2 can be observed from Fig. 3, which shows that the split-ring feeding line can generate two orthogonal modes with 90 phase difference and achieve CP radiation at the lower band (2.2 GHz). In addition, the introduced inner split-ring can not only enhance the impedance bandwidth from 54.5% (Ant 1) with the center frequency of 2.75 GHz to 63.3% (Ant 2) with the center frequency of 3 GHz, but also achieve CP radiation at the upper band (3.8 GHz). This phenomenon has been studied with current distribution, as shown in Fig. 4.

As shown in Fig. 4, the simulated time-varying surface current distributions of the proposed antenna can be employed to explain the CP radiation principle. The current distributions in the figure are viewed from the $+z$ direction, showing the direction of the distributed current at different time phases (w_t), from 0° to 270°, with an interval of 90°. In this figure, it is obvious that the current of the square slot travels in the clockwise direction as w_t increases (Fig. 4(a)) in the proposed antenna 2, which results in a LHCP radiation, and the current of the split-rings travels in the counterclockwise direction as w_t increases (Fig. 4(b)) in the proposed antenna 2, which results in a RHCP radiation.

3. SIMULATION AND RESULTS

3.1. S-Parameters

The antenna performance is first investigated by the EM full-wave simulator HFSS version 13.0. The measurements are carried out using Agilent 8753E network analyzer. As shown in Fig. 5, the simulated and measured $|S_{11}|$ of the proposed antenna are less than -10 dB over the frequency range of $2.0 \sim 3.9$ GHz (63.3%). The manufacture errors affect the impedance of the antenna, which may lead to the disagreement between simulations and measurements. The measured results of $|S_{11}|$ show good agreement with the simulated results.

3.2. Radiation Patterns

The proposed antenna is measured in an anechoic chamber. The simulated and measured AR and LHCP/RHCP radiation patterns are plotted in Fig. 6 and Fig. 7. The measured results in Fig. 6 show that the 3-dB AR bandwidths in the lower and upper bands are 9.8% ($2.12 \sim 2.34$ GHz) and 5.1% ($3.67 \sim 3.86$ GHz), respectively. Fig. 7 shows the radiation patterns in XOZ plane and YOZ plane of the proposed antenna at 2.2 GHz and 3.8 GHz. As shown in Fig. 7, the proposed antenna exhibits good

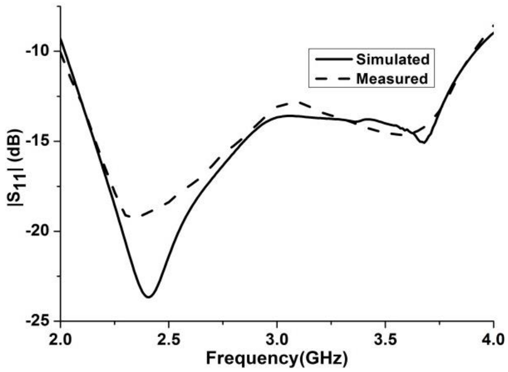

Figure 5. $|S_{11}|$ of the proposed dual-band dual-sense CP antenna.

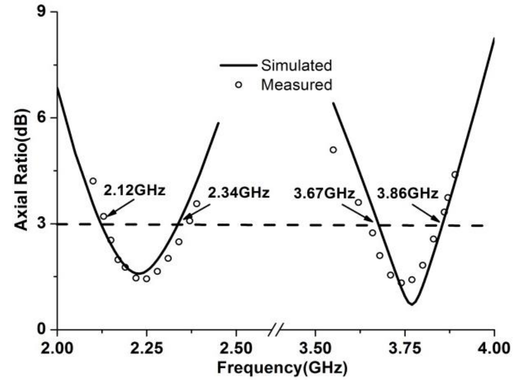

Figure 6. AR of the proposed dual-band dual-sense CP antenna.

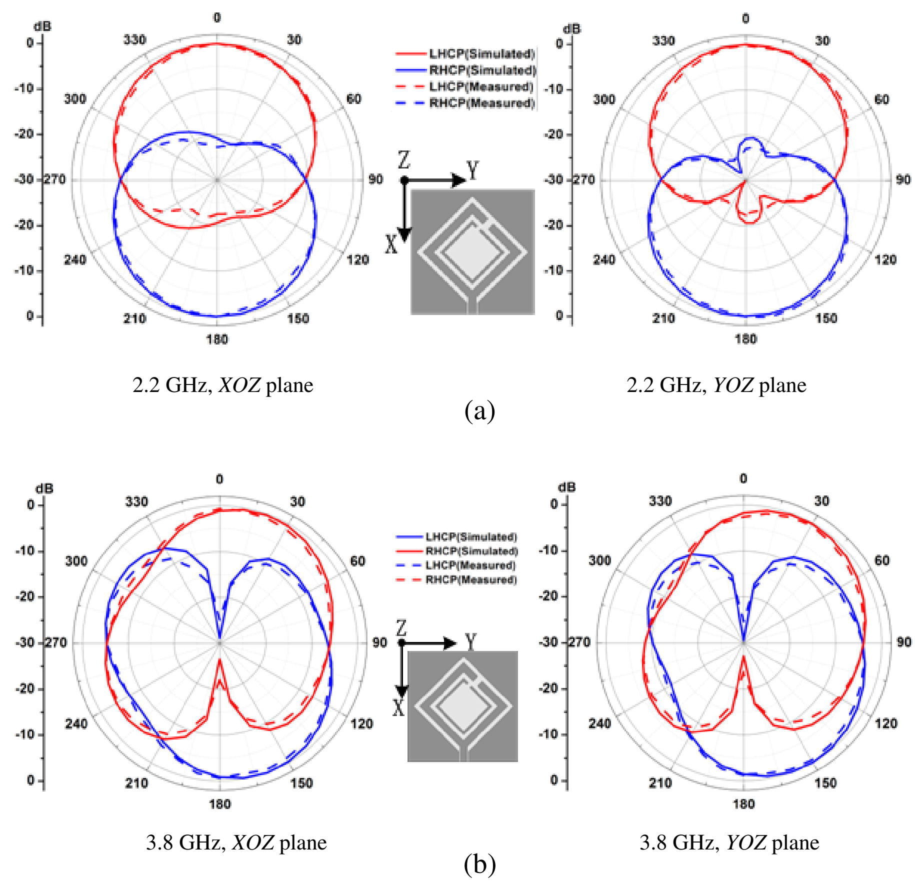

Figure 7. LHCP/RHCP radiation patterns of the proposed antenna in XOZ and YOZ planes. (a) 2.2 GHz, (b) 3.8 GHz.

circular polarization performance with cross polarization level better than 20 dB. It has bidirectional radiation pattern with a slight angle shift in its main direction, which is mainly due to the external feeding structure of the antenna. Fig. 8(a) shows the measured peak gains of the proposed antenna. The measured results show that the peak gains of the proposed antenna in the direction of the main beam are 3.2 dBic at 2.2 GHz (LHCP) and 2.1 dBic at 3.8 GHz (RHCP). As shown in Fig. 8(b), the overall radiation efficiency of the antenna operated in the two CP bands is above 85%.

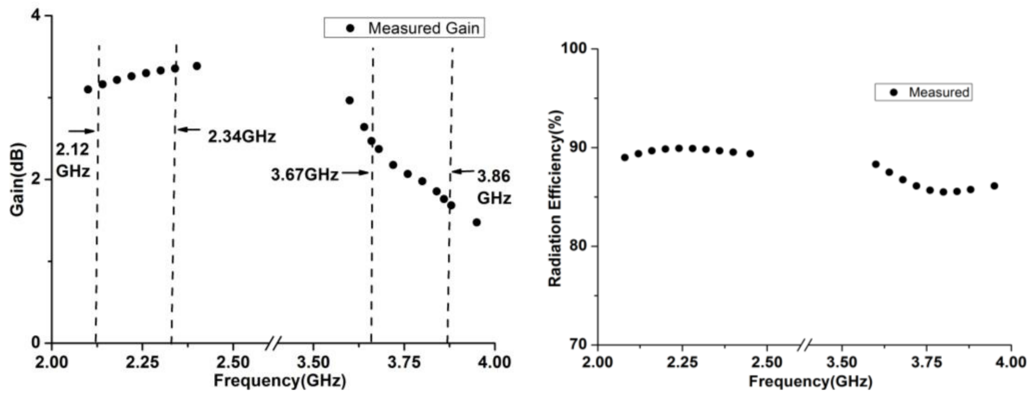

(a) (b)

Figure 8. Measured peak gain and radiation efficiency of the proposed antenna: (a) Gain, (b) radiation efficiency.

4. PARAMETRIC STUDY

All critical physical parameters, such as L_1, L_2, L_3, L_4 and W_3, should be adjusted carefully in order to achieve a dual-band dual-sense CP design with good performance. In this section, we will examine the effects of these parameters on impedance bandwidth and AR with only one parameter varying at a time.

As mentioned prior that the lower CP resonance frequency is decided by the split-ring feeding line and the upper CP resonance frequency is decided by the introduced inner split-ring, so it is obvious that the size of the outer split-ring (L_1) can affect the lower frequency while the size of the inner split-ring (L_3) can influence the upper one.

4.1. Effects of L_2

The effects of the location of the gap in the split-ring feeding-line L_2 on the impedance bandwidth and AR of the proposed antenna are shown in Figs. 9(a) and (b), respectively. It is noted that with an increase of L_2 from 7 to 9 mm, the impedance of upper band becomes better, while the CP resonance frequency of lower band decreases. Whether the value of L_2 is too small or too large, the impedance of lower band and AR of upper band will be deteriorated. To obtain good impedance matching and CP performance, L_2 should be set to be 9 mm.

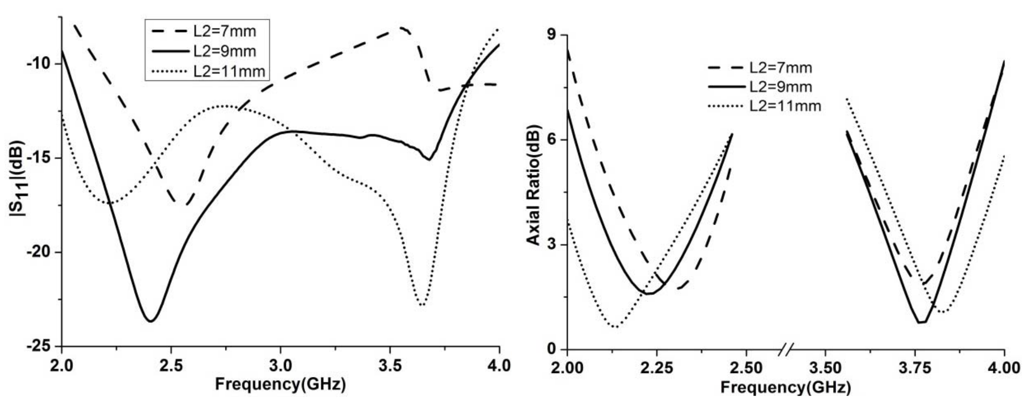

(a) (b)

Figure 9. Simulated $|S_{11}|$ and AR with different L_2's for the proposed dual-band dual-sense antenna. (a) $|S_{11}|$, (b) AR.

4.2. Effects of L_4

Figure 10 shows the effects of L_4, which is the location of the gap in the inner split-ring. As expected, L_4 has little effect on the impedance bandwidth. To realize AR at both of the operating bands, L_4 must be optimized. Whether the value of L_4 is too small or too large, the AR matching will be deteriorated. To obtain good AR, L_4 should be set as 2 mm.

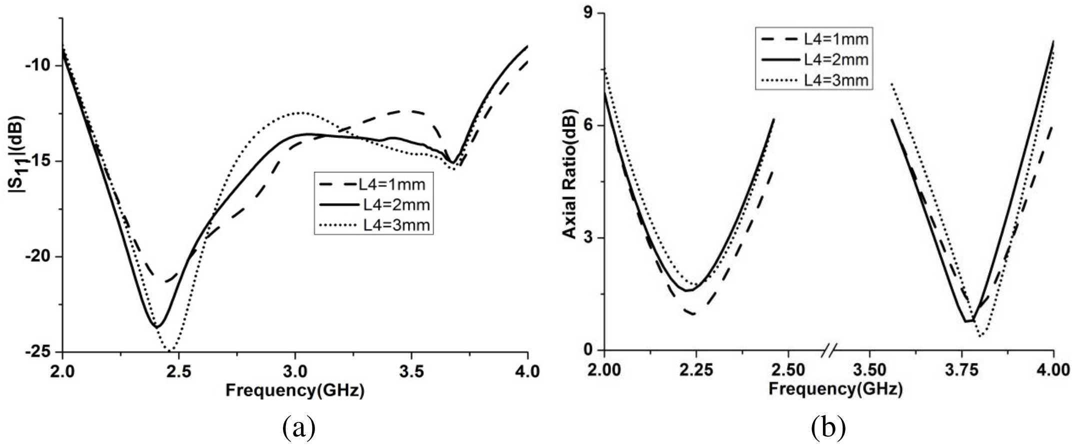

Figure 10. Simulated $|S_{11}|$ and AR with different L_4's for the proposed dual-band dual-sense antenna. (a) $|S_{11}|$, (b) AR.

4.3. Effects of W_3

Figure 11 shows the effects of W_3, which is the width of the inner ring. It is noted that W_3 mainly affect the impedance bandwidth of both frequency, while AR is slightly affected. To realize impedance matching at both of the operating bands, W_3 must be optimized. Whether the value of W_3 is too small or too large, the impedance matching will be deteriorated. To obtain good impedance matching, W_3 should be set as 1 mm.

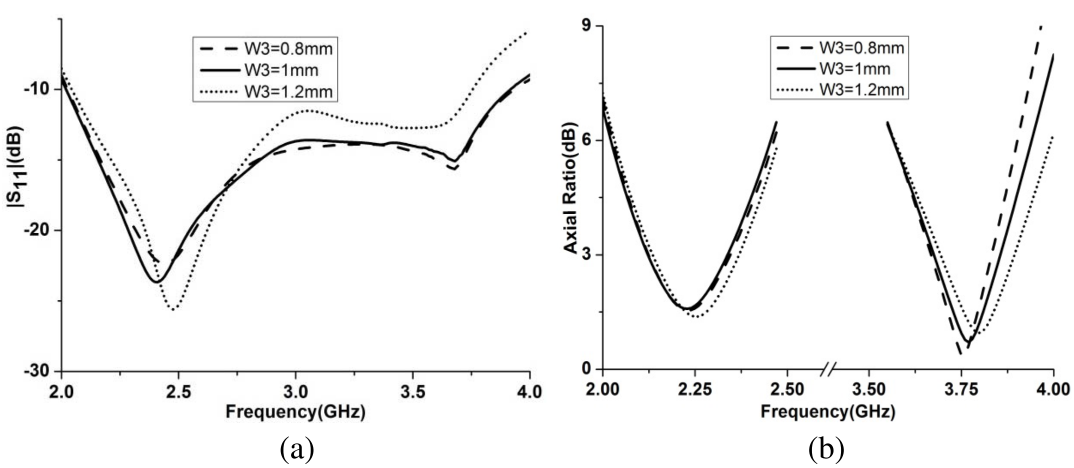

Figure 11. Simulated $|S_{11}|$ and AR with different W_3's for the proposed dual-band dual-sense antenna. (a) $|S_{11}|$, (b) AR.

5. CONCLUSIONS

A novel planar compact dual-band dual-sense circularly polarized (CP) metal-strip antenna is proposed. By appropriately introducing dual split-ring elements, the proposed dual-band CP design can easily be achieved with the impedance bandwidth ($|S_{11}| \leq -10\,\text{dB}$) of $2.0 \sim 3.9$ GHz and the 3 dB axial-ratio (AR) bandwidth of about 220/190 MHz for 2.2/3.8 GHz. The measured peak gain and radiation efficiency are about 3.2/2.1 dBic and 94/84% across the operating band, respectively, with nearly bidirectional patterns in the XZ- and YZ-plane.

REFERENCES

1. Bao, X. and M. J. Ammann, "Dual-frequency dual-sense circularly-polarized slot antenna fed by microstrip line," *IEEE Transactions on Antennas and Propagation*, Vol. 56, No. 3, 645–649, 2008.
2. Bao, X. L. and M. J. Ammann, "Monofilar spiral slot antenna for dual-frequency dual-sense circular polarization," *IEEE Transactions on Antennas and Propagation*, Vol. 59, No. 8, 3061–3065, 2011.
3. Chen, Y.-Y., et al., "Dual-band dual-sense circularly polarized slot antenna with a C-shaped grounded strip," *IEEE Antennas and Wireless Propagation Letters*, Vol. 10, 915–918, 2011.
4. Chen, C. and E. K. N. Yung, "Dual-band dual-sense circularly-polarized CPW-fed slot antenna with two spiral slots loaded," *IEEE Transactions on Antennas and Propagation*, Vol. 57, No. 6, 1829–1833, 2009.
5. Lee, B., et al., "Dual-band dual-circularly-polarized sector antenna for GPS and DAB systems," *Microwave and Optical Technology Letters*, Vol. 46, No. 1, 43–46, 2005.
6. Rezaeieh, S. A., "Dual band dual sense circularly polarised monopole antenna for GPS and WLAN applications," *Electronics Letters*, Vol. 47, No. 22, 1212–1214, 2011.
7. Lei, Z. Y., J. Zhang, R. Yang, X. Liu, L. Chen, and X. Kong, "Design of dual-band dual-sense circularly polarized slot antenna," *Progress In Electromagnetics Research C*, Vol. 43, 41–51, 2013.
8. Shao, Y. and Z. Chen, "A design of dual-frequency dual-sense circularly-polarized slot antenna," *IEEE Transactions on Antennas and Propagation*, Vol. 60, No. 11, 4992–4997, 2012.
9. Sze, J.-Y., T.-H. Hu, and T.-J. Chen, "Compact dual-band annular-ring slot antenna with meandered grounded strip," *Progress In Electromagnetics Research*, Vol. 95, 299–308, 2009.
10. Shi, L., H.-J. Sun, W.-W. Dong, and X. Lv, "A dual-band multifunction carborne hybrid antenna for satellite communication relay system," *Progress In Electromagnetics Research*, Vol. 95, 329–340, 2009.
11. Lee, Y.-C. and J.-S. Sun, "Compact printed slot antennas for wireless dual-and multi-band operations," *Progress In Electromagnetics Research*, Vol. 88, 289–305, 2008.
12. Wong, K.-L., *Compact and Broadband Microstrip Antennas*, Vol. 168, John Wiley & Sons, 2004.
13. Zainud-Deen, S. H., H. A. El-Azem Malhat, and K. H. Awadalla, "A single-feed cylindrical superquadric dielectric resonator antenna for circular polarization," *Progress In Electromagnetics Research*, Vol. 85, 409–424, 2008.
14. Sorbello, R. M., et al., "A high-efficiency flat plate array for direct broadcast satellite applications," *18th European IEEE Microwave Conference*, 295–299, 1988.
15. Sorbello, R. M. and A. I. Zaghloul, "Wideband, high-efficiency, circularly polarized slot elements," *AP-S. Digest. IEEE Antennas and Propagation Society International Symposium*, Vol. 3, 1473–1476, 1989.
16. Jun, J. and Y. Lee, "Triplate printed antenna with circular slot," *IEEE Antennas and Propagation Society International Symposium*, Vol. 4, 2128–2130, 1998.
17. Chang, T. N. and C.-P. Wu, "Microstripline-fed circularly-polarized aperture antenna," *IEEE Antennas and Propagation Society International Symposium*, Vol. 3, 1372–1375, 1998.
18. Wong, K.-L., J.-Y. Wu, and C.-K. Wu, "A circularly-polarized patch loaded square-slot antenna," *Microwave and Optical Technology Letters*, Vol. 23, No. 6, 363–365, 1999.

19. Kishk, A. A., et al., "Microstrip line and CPW FED ultra wideband slot antennas with U-shaped tuning stub and reflector," *Progress In Electromagnetics Research*, Vol. 56, 163–182, 2006.
20. Jiao, J.-J., et al., "A broadband CPW-fed T-shape slot antenna," *Progress In Electromagnetics Research*, Vol. 76, 237–242, 2007.
21. Si, L.-M. and X. Lv, "CPW-FED multi-band omni-directional planar microstrip antenna using composite metamaterial resonators for wireless communications," *Progress In Electromagnetics Research*, Vol. 83, 133–146, 2008.
22. De Villiers, J. P. and J. P. Jacobs, "Gaussian process modeling of CPW-FED slot antennas," *Progress In Electromagnetics Research*, Vol. 98, 233–249, 2009.
23. Liu, X. L., Y.-Z. Yin, P. A. Liu, J. H. Wang, and B. Xu, "A CPW-fed dual band-notched UWB antenna with a pair of bended dual-L-shape parasitic branches," *Progress In Electromagnetics Research*, Vol. 136, 623–634, 2013.
24. Saed, M. A., "Broadband CPW-fed planar slot antennas with various tuning stubs," *Progress In Electromagnetics Research*, Vol. 66, 199–212, 2006.
25. Chen, C. H. and E. K. N. Yung, "Dual-band circularly-polarized CPW-fed slot antenna with a small frequency ratio and wide bandwidths," *IEEE Trans. Antennas Propag.*, Vol. 59, No. 4, 1379–1384, Apr. 2011.
26. Li, Q., et al., "A single-feed dual-band dual-sense circularly polarized microstrip antenna," *Progress In Electromagnetics Research C*, Vol. 51, 27–33, 2014.
27. Shao, Y. and Z. Chen, "A design of dual-frequency dual-sense circularly-polarized slot antenna," *IEEE Transactions on Antennas and Propagation*, Vol. 60, No. 11, 4992–4997, 2012.